Isolation and Characterization of Four Isomers of a C_{60} Bisadduct with a TTF Derivative. Study of Their Radical Ions

M. Mas-Torrent,[†] R. A. Rodríguez-Mias,[‡] M. Solà,[‡] M. A. Molins,[⊥] M. Pons,[§] J. Vidal-Gancedo,[†] J. Veciana,[†] and C. Rovira*,[†]

Institut de Cìencia de Materials de Barcelona (CSIC), Campus Universitari de Bellaterra, 08193 Cerdanyola, Spain, Institut de Química Computacional, i Departament de Química, Universitat de Girona, Campus Montilivi, 17071 Girona, Spain, Departament de Química Orgànica, Facultat de Química, Universitat de Barcelona, Martí i Franquès 1, 08028 Barcelona, Spain, and Serveis Cientificotècnics, Lluís Solė i Sabarís, 08028 Barcelona, Spain

cun@icmab.es

Received July 25, 2001

A family of triads composed of C_{60} attached by a rigid spacer to two identical TTF moieties has been synthesized, and some of the isomers have been isolated and characterized by UV-vis spectroscopy, LDI-TOF-MS, and HMBC NMR spectroscopy. AM1 semiempirical calculations of the dipolar moments and the heats of formation of the different isomers have been carried out in order to verify their assignments. Oxidation and reduction of the triads affords the derived radical ion systems, $TTF^{+\bullet}-C_{60}-TTF^{+\bullet}$ and $TTF-C_{60}^{-\bullet}-TTF$, which were studied by EPR spectroscopy. Spin density distributions of these radical cations and radical anions show that the unpaired electron is located mainly on the TTF and fullerene moieties, respectively. However, while the EPR signals obtained from the radical cations are very similar for all the isomers, the structured signals observed for the radical anions arising from the coupling of the unpaired electron with the hydrogen atoms of the methylene bridges in the spacer show that there is a strong influence of the isomerism on the spin distribution. Importantly, the theoretical calculations of the spin density distributions of the radical anions fit well with the experimental EPR results.

Introduction

C_{60} appears to undergo reactions associated with poorly conjugated electron-deficient alkenes. However, a unique feature of C_{60} is that a large number of products may arise from polyaddition since it has 30 reactive [6,6] double bonds. Polyadducts of C_{60} with well-defined three-dimensional structure are of great importance as they possess biological[1a] and material properties.[1b,c] Up to now, several electron donors such as porphyrins, ferrocenes, tetrathiafulvalenes (TTFs), and phthalocyanines have been attached to the fullerene cage,[2−13] and, in a few cases, the final compounds show interesting intra-molecular electronic interactions between the C_{60} and the addends. Some of these donor−acceptor dyads form long-lived charge-separated species upon irradiation[9−12] and therefore are interesting systems as molecular building blocks in electrooptical and photovoltaic devices, as well as bistable molecular information storage units.[14]

We have been working with dyads composed of TTF derivatives linked to a C_{60} moiety by a bismethylene bridge, obtained through a Diels−Alder reaction, in which photoexcitation of the fullerene moiety leads to

---

* Corresponding author. Phone: +(34)-935801853 extn. 245; Fax: +(34)-935805729;.
† Institut de Cìencia de Materials de Barcelona (CSIC).
‡ Universitat de Girona.
§ Universitat de Barcelona.
⊥ Serveis Cientificotècnics.
(1) (a) Friedman, S. H.; De Camp, D. L.; Sijbesma, R. P.; Srdanov, G.; Wudl, F.; Kenyon, G. L. *J. Am. Chem. Soc.* **1993**, *115*, 6506. (b) Hirsch, A. *Adv. Mater.* **1993**, *5*, 859. (c) Prato, M. *J. Mater. Chem.* **1997**, *7*, 1097.
(2) (a) Rubin, Y.; Khan, S.; Freedberg, D. I.; Yeretzian, C. *J. Am. Chem. Soc.* **1993**, *115*, 344. (b) Rubin, Y.; Khan, S. I.; Oliver, A. M.; Paddon-Row, M. N. *J. Am. Chem. Soc.* **1993**, *115*, 4919. (c) Mullen, K.; Belik, P.; Gügel, A.; Spickermann, J. *Angew. Chem., Int. Ed. Engl.* **1993**, *32*, 78. (d) Liddell, P.; Mcpherson, A. N.; Sumida, J.; Demanche, L.; Moore, A. L.; Moore, T. A.; Gust, D. *Photochem. Photobiol.* **1994**, *595*, 365. (e) Linssen, T. G.; Dürr, K.; Hannack, M.; Hirsch, A. *J. Chem. Soc., Chem. Commun.* **1995**, 103.
(3) Matsubara, Y.; Tada, H.; Nagase, S.; Yoshida, Z. *J. Org. Chem.* **1995**, *60*, 5372.
(4) Isaacs, L.; Haldimann, T. G.; Diederich, F. *Angew. Chem. Int. Ed. Engl.* **1994**, *33*, 2339.
(5) Boulle, C.; Rabreau, J.-M.; Hudhomme, P.; Cariou, M.; Jubault, M.; Gorgues, A.; Orduna, J.; Garín, J. *Tetrahedron Lett.* **1997**, *38*, 3909.
(6) Imahori, H.; Sakata, Y. *Adv. Mater.* **1997**, *9*, 537.
(7) Martín, N.; Sánchez, L.; Illescas, B.; Pérez, I. *Chem. Rev.* **1998**, *98*, 2527.

(8) (a) Lawson, J. M.; Oliver, A. M.; Rothenfluh, D. F.; An, Y.-Z.; Ellis, G. A.; Ranasinghe, M. G.; Khan, S. I.; Franz, A. G.; Ganapathi, P. S.; Shephard, M. J.; Paddon-Row, M. N.; Rubin, Y. *J. Org. Chem.* **1996**, *61*, 5032. (b) Liddell, P. A.; Kuciauskas, S.; Sumida, J. P.; Nash, B.; Nguyen, D.; Moore, A. L.; Moore, T. A.; Gust, D. *J. Am. Chem. Soc.* **1997**, *119*, 1400. (c) Guldi, D. M.; Maggini, M.; Scorrano, G.; Prato, M. *J. Am. Chem. Soc.* **1997**, *119*, 974. (d) Boulle, C.; Rabreau, S.-M.; Hudhomme, P.; Cariou, M.; Jubault, M.; Gorgues, A.; Orduna, J.; Garin, J. *Tetrahedron Lett.* **1997**, *38*, 3909.
(9) (a) Imahori, H.; Sakata, Y. *Eur. J. Org. Chem.* **1999**, 2445. (b) Fujitsuka, M.; Ito, O.; Imahori, H.; Yamada, K.; Yamada, H.; Sakata, Y. *Chem. Lett.* **1999**, 721.
(10) Llacay, J.; Veciana, J.; Vidal-Gancedo, J.; Bourdelande, J. L.; González-Moreno, R.; Rovira, C. *J. Org. Chem.* **1998**, *63*, 5201.
(11) (a) Guldi, D. M.; González, S.; Martín, N.; Antón, A.; Garín, J.; Orduna, J. *J. Org. Chem.* **2000**, *65*, 1978. (b) Martín, N.; Sánchez, L.; Hernanz, M. A.; Guldi, D. M. *J. Phys. Chem.* **2000**, *104*, 4648.
(12) (a) Guldi, D. *Chem. Commun.* **2000**, 321. (b) Guldi, D. M.; Luo, C.; Da Ros, T.; Prato, M.; Dietel, E.; Hirsch, A. *Chem. Commun.* **2000**, 375. *Ibid.* 373.
(13) (a) Prato, M.; Maggini, M.; Giacometti, C.; Scorrano, G.; Sandonà, G.; Farina, G. *Tetrahedron* **1996**, *52*, 5221. (b) Martín, N.; Sánchez, L.; Seoane, C.; Andreu, R.; Garín, J.; Orduna, J. *Tetrahedron Lett.* **1996**, *37*, 5979. (c) Martín, N.; Pérez, I.; Sánchez, L.; Seoane, C. *J. Org. Chem.* **1997**, *62*, 5690.
(14) (a) Sariciftci, N. S.; Smilowitz, L.; Heeger, A. J.; Wudl, F. *Science* **1992**, *258*, 1474. (b) Yu, G.; Pakbaz, K.; Heeger, A. J. *Appl. Phys. Lett.* **1994**, *64*, 3422.

Chart 1

$n = 1; 2$
$n = 2; 3$
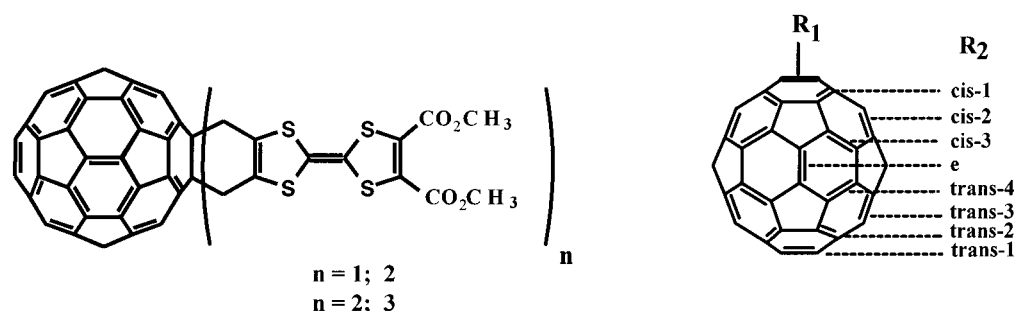
transient charge-separated open-shell species with very long lifetimes.[10] In these dyads, the C_{60} electron acceptor and the TTF electron donor are directly united by two rigid σ bonds which provide not only short separation but also a rigid bridge between them and therefore a well-defined relative distance and orientation.

The synthesis of triads ($C_{60}R_2$) is of great interest for studying the influence of the isomerism on the physical properties,[15–27] despite the fact that there are not many precedents due to the laborious task of isolation and characterization of the isomers. As crystals of these compounds suitable for X-ray structure determination are usually difficult to obtain,[28,29] the assignment of the correct structure for all the isomers has become an important aim, and several groups have been seeking a systematic method to characterize them. Different criteria, such as polarity and UV-vis and NMR spectroscopic data, have been commonly used to imply their nature. Wilson and Schuster have also attempted to correlate the structure of bisadducts exploiting the ^{3}He chemical shifts in the NMR spectra of ^{3}He@C_{60} fullerene derivatives,[16] and Pasimeni et al. suggested a new method based on

an EPR study of the excited triplet state of the bisadducts.[21] It has been also shown previously that INADEQUATE NMR[30] and HMBC NMR[31] are useful tools in their characterization.

Herein, we report the study of a family of triads formed by two identical TTF moieties attached to the fullerene cage **3** (Chart 1). The electrochemically generated radical ion systems, $TTF^{+•}–C_{60}–TTF^{+•}$ and $TTF–C_{60}^{-•}–TTF$, show interesting features regarding the influence of the isomerism on the spin distribution in the molecules. Moreover, an extended theoretical study by means of semiempirical and density functional methods has also been carried out in order to interpret the experimental observations, in particular the order of elution in chromatography and the EPR spectra.

Results and Discussion

Synthesis and Characterization of the Bisadducts. A Diels–Alder reaction was used for the synthesis of the triad **3**, which was achieved either by direct bisaddition of the diene, generated upon elimination of SO_2 from bis(methoxycarbonyl)-3-sulfolene-tetrathiafulvalene **1**, to the fullerene[10] or by a second cycloaddition to the monoadduct **2** (Scheme 1). In the former reaction, a mixture of nonreacted C_{60}, monoadduct **2**, and bisadducts **3** was obtained, which were separated by column chromatography. The isolated monoadduct **2** was used as a reagent for the second synthetic pathway, in which the mixture of isomers of **3** was also separated from the nonreacted monoadduct **2** and polyadducts by column chromatography. Depending on the relative position of the addends in the fullerene cage, eight regioisomers can be formed (Chart 1), which were detected by analytical HPLC on silica gel as stationary phase and 0.3% AcOEt in CH_2Cl_2 as mobile phase (Figure 1). Further separation of the very insoluble mixture of regioisomers with a semipreparative silica column enabled the isolation of a few milligrams of four of the isomers, **3a**, **3c**, **3e**, and **3f**. The laser desorption–ionization time-of-flight (LDI-TOF) mass spectra of all of them as well as of those corresponding to the other chromatographic peaks show the molecular peak at m/z 1412, which confirms that they are isomers of **3**. However, it is worth pointing out that the fraction corresponding to the last peak in the chromatogram **3h** should be attributed to a trisadduct, as a low intensity peak at m/z 1759 was observed. We want to highlight that the difficult task of isomer separation

(15) Lu, Q.; Schuster; D. I.; Wilson, S. R. *J. Org. Chem.* **1996**, *61*, 4764–4768.

(16) Cross, J.; Jiménez-Vázquez, H. A.; Lu, Q.; Saunders, M.; Schuster, D. I.; Wilson, S. R.; Zhao, H. *J. Am. Chem. Soc.* **1996**, *118*, 11454.

(17) Schick, G.; Hirsch, A.; Mauser, H.; Clark, T. *Chem. Eur. J.* **1996**, *2*, 935.

(18) Hirsch, A.; Lamparth, I.; Karfunkel, H. R. *Angew. Chem., Int. Ed. Engl.* **1994**, *33*, 437.

(19) Djojo, F.; Herzog, A.; Lamparth, I.; Hampel, F.; Hirsch, A. *Chem. Eur. J.* **1996**, *2*, 1537.

(20) Djojo, F.; Hirsch, A. *Chem. Eur. J.* **1998**, *4*, 344.

(21) Pasimeni, L.; Hirsch, A.; Lamparth, I.; Herzog, A.; Maggini, M.; Prato, M.; Corvaja, C.; Scorrano, G. *J. Am. Chem. Soc.* **1997**, *119*, 12896.

(22) (a) Taki, M.; Sugita, S.; Nakamura, Y.; Kasashima, E.; Yashima, E.; Okamoto, Y.; Nishimura, J. *J. Am. Chem. Soc.* **1997**, *119*, 926. (b) Nakamura, Y.; Asami, A.; Inokuma, S.; Ogawa, T.; Kikuyama, M.; Nishimura, J. *Tetrahedron Lett.* **2000**, *41*, 2193. (c) Nakamura, Y.; O-kawa, K.; Matsumoto, M.; Nishimura, J. *Tetrahedron* **2000**, *56*, 5429. (d) Nakamura, Y.; Tacano, N.; Nishimura, T.; Yashima, E.; Sato, M.; Kudo, T.; Nishimura, J. *Org. Lett.* **2001**, *3*, 1193. (e) Ishi-I, T.; Shinkai, S. *Tetrahedron* **1999**, *55*, 12515.

(23) Beulen, M. W. J.; Rivera, J. A.; Herranz, M. A.; Illescas, B.; Martín, N.; Echegoyen, L. *J. Org. Chem.* **2001**, *66*, 4393.

(24) Diederich, F.; Kessinger, R. *Acc. Chem. Res.* **1999**, *32*, 537.

(25) (a) Nakamura, Y.; Taki, M.; Tobita, S.; Shizuka, H.; Yokoi, H.; Ishiguro, K.; Sawaki, Y.; Nishimura, J. *J. Chem. Soc., Perkin Trans. 2* **1999**, 127. (b) Sun, Y.-P.; Guduru, R.; Lawson, G. E.; Mullins, J. E.; Guo, Z.; Quinlan, J.; Bunker, C. E.; Gord, J. R. *J. Phys. Chem. B* **2000**, *104*, 4625.

(26) (a) Da Ros, T.; Prato, M.; Lucchini, V. *J. Org. Chem.* **2000**, *65*, 4289. (b) Kordatos, K.; Bosi, S.; Da Ros, T.; Zambon, A.; Lucchini, V.; Prato, M. *J. Org. Chem.* **2001**, *66*, 2802.

(27) Kreher, D.; Liu, S.-G.; Cariou, M.; Hudhomme, P.; Gorgues, A.; Mas, M.; Veciana, J.; Rovira, C. *Tetrahedron Lett.* **2001**, *42*, 3447.

(28) Woods, C. R.; Bourgeois, J.-P.; Seiler, P.; Diederich, F. *Angew. Chem., Int. Ed.* **2000**, *39*, 3813.

(29) Kadish, K. M.; Gao, X.; Van Caemelbecke, E.; Suenobu, T.; Fukuzumi, S. *J. Am. Chem. Soc.* **2000**, *122*, 563.

(30) Burley, G. A.; Keller, P. A.; Pyne, S. G.; Ball, G. E. *Chem. Commun.* **2000**, 1717.

(31) Mas-Torrent, M.; Pons, M.; Molins, M. A.; Veciana, J.; Rovira, C. *Synth. Met.* **2001**, *123*, 523.
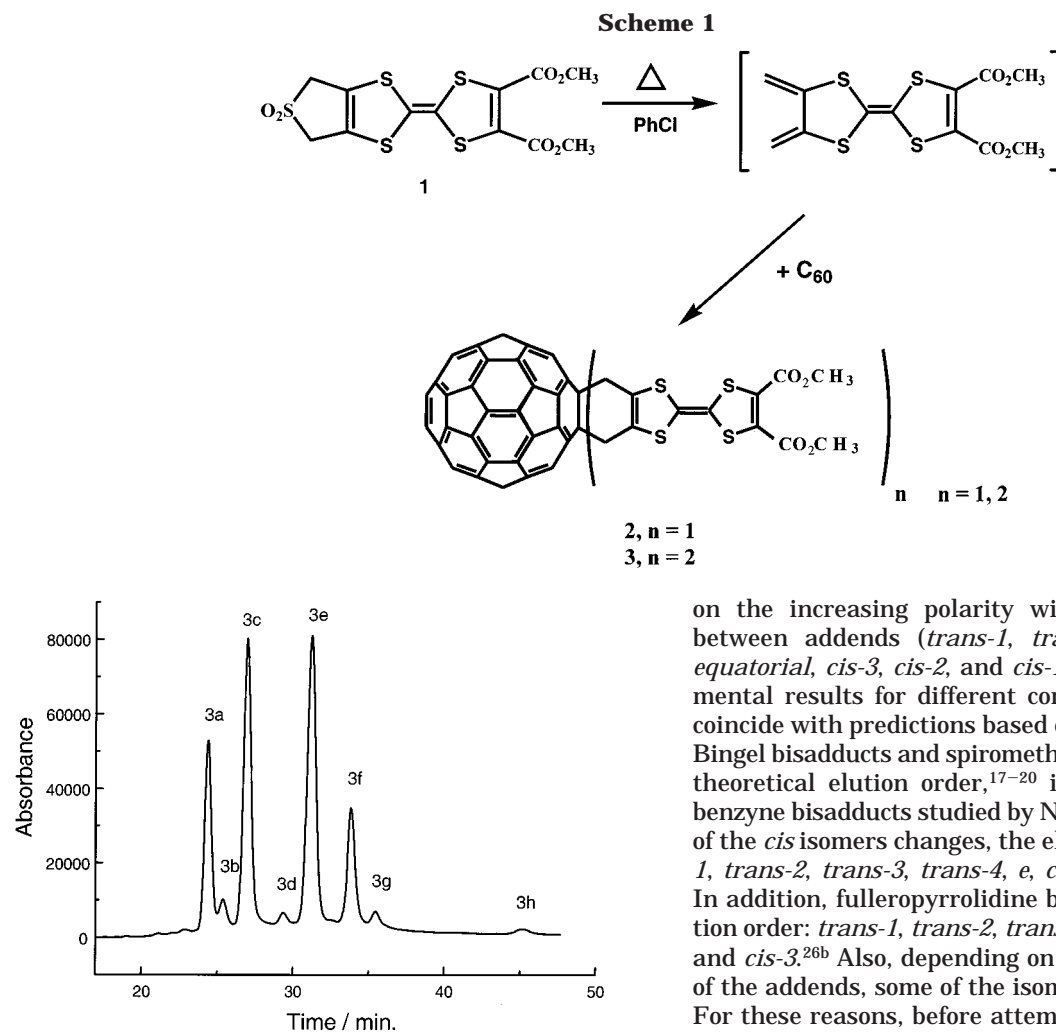
J. Org. Chem., Vol. 67, No. 2, 2002

Mas-Torrent et al.

Scheme 1

Figure 1. HPLC chromatogram of the mixture of isomeric bisadducts of **1**. Conditions: 25×0.46 cm Spherisorf Silica column, 0.3% AcOEt in CH_2Cl_2 (1 mL/min), UV-vis detection at 290 nm.

was confounded by the formation of aggregates in the solvents required to have a good separation (CH_2Cl_2/ AcOEt). It is well-known that C_{60} forms aggregates through intermolecular $\pi-\pi$ interactions,[32] resulting in broad peaks in the HPLC chromatogram and making it difficult to attain pure isomers. This problem was partially solved by treating the sample, prior to the injection in the HPLC column, with aromatic solvents such as toluene or chlorobenzene, as $\pi-\pi$ interactions of solvent molecules with the C_{60} compounds destroys the aggregates. However, the complete disaggregation of the sample is not possible, and therefore the isolation of the last eluted isomers in a pure state is extremely challenging, to the point that the last HPLC-eluted isomers are often contaminated with the first ones. The structure of the isomers corresponding to the different fractions were assigned by UV-vis spectroscopy, HMBC spectroscopy, and using polarity arguments.

At first glance, the order of elution expected in the HPLC (silica gel) for the regioisomers of **3** can be based

on the increasing polarity with decreasing distance between addends (*trans-1*, *trans-2*, *trans-3*, *trans-4*, *equatorial*, *cis-3*, *cis-2*, and *cis-1*). Nevertheless, experimental results for different compounds do not always coincide with predictions based on this argument. While Bingel bisadducts and spiromethano fullerenes follow the theoretical elution order,[17−20] in the Diels−Alder and benzyne bisadducts studied by Nishimura et al. the order of the *cis* isomers changes, the elution order being *trans-1*, *trans-2*, *trans-3*, *trans-4*, *e*, *cis-1*, *cis-2*, and *cis-3*.[22c,d] In addition, fulleropyrrolidine bisadducts show the elution order: *trans-1*, *trans-2*, *trans-3*, *cis-1*, *trans-4*, *e*, *cis-2* and *cis-3*.[26b] Also, depending on the steric requirements of the addends, some of the isomers can be less favored. For these reasons, before attempting the assignment of regioisomers of **3**, we performed semiempirical calculations of their dipolar moments as well as their heats of formation.

Since it was found that heat of formation of *cis-2* and *cis-1* isomers in their most stable conformations was higher in energy by about 8 and 15 kcal mol^{-1}, respectively, than those required for the formation of the rest of the isomers (*trans-1*, *trans-2*, *trans-3*, *trans-4*, *e*, and *cis-3*), we did not include them in the following calculations. For each isomer, four conformations arising from to the boat-to-boat inversion are possible. Previous works[2a,33] have shown that the energy barrier for the boat-to-boat inversion in C_{60} is relatively low (about 15 kcal mol^{-1}), and therefore one can expect that at room temperature there is a rapid equilibrium taking place between all possible conformers. Furthermore, the rotation of the methoxycarbonyl groups leads to additional conformers. Calculations indicate that the most stable conformations are those having the two methoxycarbonyl groups in one TTF unit located perpendicularly (see Figure 2). One group remains planar with respect to the TTF unit, taking benefit of the additional conjugation, while the other is placed perpendicularly due to steric hindrance. Taking into account this fact, four possible conformers due to rotation of the methoxycarbonyl groups for each TTF unit are possible. Overall, we have considered six different regioisomers and for each of them we

(32) (a) Ahn, J. S.; Suzuki, K.; Iwasa, Y.; Otsuka, N.; Mitani, T. *J. Luminisc.* **1998**, *76−7*, 201. (b) Nath, S.; Pal, H.; Palit, D. K.; Sapre, A. V.; Mittal, J. P. *J. Phys. Chem. B* **1998**, *102*, 10158. (c) Rudalevige, T.; Francis, A. H.; Zand, R. *J. Phys. Chem. A* **1998**, *102*, 9797. (d) Thomas, K. G.; Biju, V.; Guldi, D. M.; Kamat, P. V.; George, M. V. *J. Phys. Chem. B* **1999**, *103*, 8864.

(33) Shepard, M. J.; Paddon-Row, M. N. *Aust. J. Chem.* **1996**, *49*, 395.
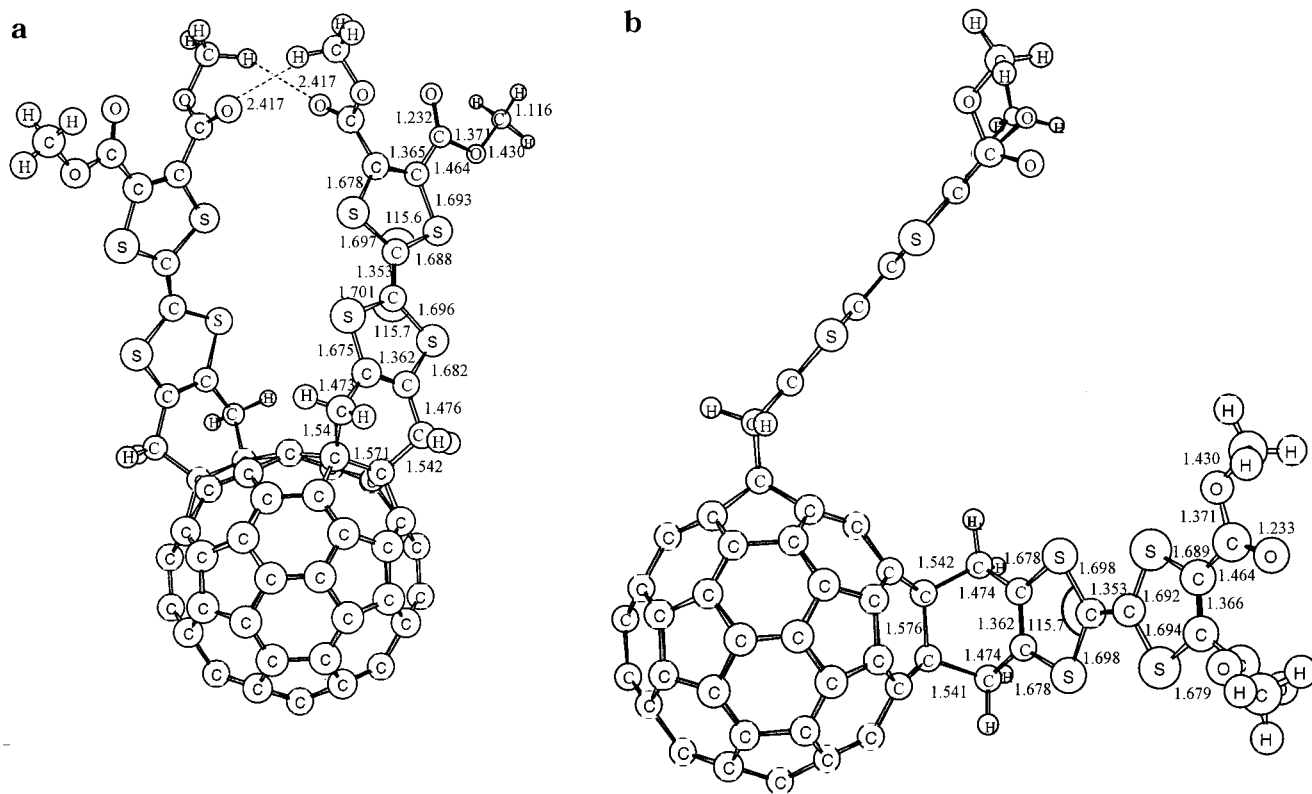
a

b

Figure 2. AM1-optimized geometry of the gas-phase most stable boat-to-boat conformer for (a) the *cis-3* regioisomer; (b) the *equatorial* regioisomer.

have considered 64 possible conformers. The only exception is the boat-to-boat conformer of the *cis-3* regioisomer depicted in Figure 2a. In this case, to avoid steric repulsion because of the proximity of the two TTF units, the two nearest methoxycarbonyl groups are located perpendicularly to the TTF units, with their carbonyl groups facing one each other. Therefore, only one possible conformer out of 16 is possible in this particular boat-to-boat conformer. As a whole, a total of 369 conformers have been calculated, although, for symmetry reasons, some of them are equivalent.

Surprisingly, it was found that the dipole moment of the isomer depends greatly on its conformation. In particular, the position of the methoxycarbonyl groups has an enormous influence on the dipole moment. For instance, the value of the dipole moment for the *trans-1* regioisomer varies from 0.00 to 6.01 D, while that of the *trans-2* isomer from 0.33 to 6.98 D. Indeed, depending on the conformation, the *trans-1* isomer can be even more polar than the *cis-3* isomer. As a consequence, for this particular derivative **3**, the use of the expected polarity (based on the relative position of the addends) to assign the order of elution without further checking is questionable. For this reason we have theoretically assigned a dipole moment to each regioisomer by computing the dipole moment of all conformers considered (for further information see the Computational Details). Table 1 gathers the values of the dipole moments obtained in this way. It is seen that the polarity found theoretically is in accordance to what was expected on the basis of relative position of the two TTF units in the fullerene core, the polarity decreasing in the order *cis*-3, e, *trans-4*, *trans-3*, *trans-2*, and *trans-1* regioisomers.

Experimentally, the synthesis of isomer **3** takes place in toluene solution at 120 °C. Given the low dielectric

Table 1. Assignment of the Chromatographic Peaks Resulting from the Separation of the Isomers of 3

peak	retention time (min)	assignment	μ calcd (D)[a]	% chromatogram peak area	% theoret abundance[b]
3a	24.40	*trans-2*	3.39	16.1	13.1
3b	25.39	*trans-1*	3.13	3.6	1.7
3c	26.99	*trans-3*	3.45	28.8	20.6
3d	29.36	*trans-4*	3.48	2.8	27.8
3e	31.24	*equatorial*	3.57	32.0	36.1
3f	33.85	*cis-3*	3.85	12.9	0.6
3g	35.50	*cis-2*	–	3.0	–
3h	45.20	*trisadduct*	–	0.8	–

[a] Dipole moment in Debeyes. [b] Product distribution at 393 K calculated by AM1 method.

constant of toluene, we have used the calculated Gibbs energy in gas phase at 393 K to calculate the theoretical relative abundances of the regioisomers, considering now a Maxwell−Boltzmann distribution of all possible conformers of the *cis*-3, e, *trans-4*, *trans-3*, *trans-2*, and *trans-1* regioisomers. The results of theoretical relative abundances together with the experimental product distribution obtained from the different HPLC chromatogram peak areas are listed in Table 1. The experimental results differ significantly from the theoretical ones, especially in the case of the *trans-4* regioisomer, indicating that the bisadduct formation probably takes place under kinetic control. A similar conclusion was also reached by Hirsch et al.[34] in the study of multiple nucleophilic cyclopropanations to the fullerene core.

It is also worth pointing out that, for each isomer, the stability of all possible conformations are quite similar, the differences among conformations of the same regio-

(34) Hirsch, A.; Lamparth, I.; Grösser, T. *J. Am. Chem. Soc.* **1994**, *116*, 9385.
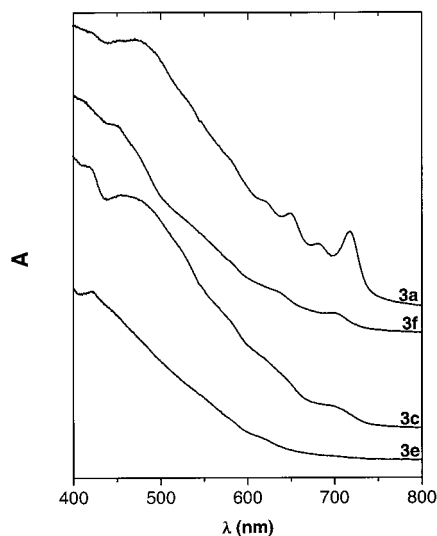
Figure 3. Visible absorption spectra of regioisomers **3a** (*trans-2*), **3c** (*trans-3*), **3e** (*equatorial*), and **3f** (*cis-3*) in CH_2Cl_2.

isomer being always smaller than 0.4 kcal mol^{-1}, with the exception of isomer *cis-3*, in which the conformation depicted in Figure 2a is more stable than the rest by about 1 kcal mol^{-1}. This gain of stability is attributed to the formation of two C−H···O hydrogen bonds between the carboxymethyl groups of the two addends. However, in solution this conformation is particularly destabilized by the proximity of the two TTF units which leads to a decrease of the total solvent accessible surface by about 100 Å^2, which in turn is responsible for the reduction of the solvation free energy of this conformer by ca. 3 kcal mol^{-1}.

On the other hand, the experimental results available at present indicate that the electronic properties of a given bisadduct depend principally on the addition pattern rather than the nature of the addend. Especially, the characteristic features in the region between 400 and 800 nm can be used as a fingerprint for the identification of a given regioisomer.[17,18] Hence, comparing the electronic spectra obtained for **3a**, **3c**, **3e**, and **3f** (Figure 3) with the ones found in the literature[15,19,22,23,26b] and taking into account the former dipole moment calculations that permit the estimation of the order of elution, it is possible to make a reasonable assignment of isomers **3a**, **3c**, **3e**, and **3f** to isomers *trans-2*, *trans-3*, *e*, and *cis-3* respectively (Table 1). Thus, the position, intensity and the width of the bands in the Visible spectrum of isomers **3a** and **3c** are almost identical to those observed for the *trans-2* and *trans-3* isomers in the bisadducts of *o*-quinodimethane,[22b] fulleropyrrodiline,[26b] and benzyne[22d] derivatives and quite similar to those reported for other bisadducts.[19,23] Isomer **3e** shows the same spectrum as those of the *equatorial* isomers of quinodimethane,[22a,c,e] and fulleropyrrodiline[26b] derivatives. The visible spectrum of isomer **3f** has the same characteristic features as those of *cis-3* isomers of of *o*-quinodimethane,[22a,b] fulleropyrrodiline,[26] and benzyne[22d] derivatives as well as anisyl and methanofullerenes.[19,23] These features are quite different from those shown by the corresponding *cis-2* isomers especially in the 600−750 nm region, thus permitting the assignment of *cis-3* isomer to **3f**.

It is worth noting that this assignment fits with the one expected according to the order of elution with the exception of the *trans-2* isomer, which elutes before *trans-*

1. However, similar changes in the elution order have also been observed in other C_{60}-bisadducts and always with those isomers that have much less abundance than the corresponding neighbors.[19,26b]

The complete characterization of the regioisomers of **3** should be performed by NMR, but good ^{1}H and ^{13}C NMR spectra were not plausible on account of the very low solubility of these compounds. Nevertheless, thanks to the use of the HMBC technique, the NMR characterization of two of them was possible, and it is in good agreement with the previous assignment of the isomers.[35] In particular, isomers **3a** (*trans-2*) and **3e** (*equatorial*) have been studied by HMBC, and the spectra obtained are in accord with their symmetry.[31] The assignment of the chemical shifts are summarized in Table 2. The unexpected low frequency of one of the protons of a methylenic group of bisadduct **3e** (H$_1$) can be attributed to ring current effects arising from the π system of the other TTF addend, that according to the theoretical structure is situated in a molecular plane almost perpendicular to the H$_1$ proton (Figure 2b). Moreover, the C_{A2} carbon atom of the same isomer and also one of the adjacent carbon atoms of the isomer **3a** resonate at ca. 160 ppm, more than 6 ppm higher than the other adjacent carbon atoms. As a matter of fact, the relative disposition of the anomalous C_A with respect to the anchoring bond of the TTF addend, along a pathway defined by two connected 5-radialene units, is the same for both *trans-2* (**3a**) and *equatorial* (**3e**) isomers. If this observation about some adjacent carbon atoms appearing at an unexpected chemical shift only in some of the isomers can be generalized, it may provide an additional simple tool for the characterization of C_{60} bisadducts. In support of this hypothesis, we note thet the C_A of *trans-2* and *equatorial* isomers of bisadducts of fulleropyrrolidine derivatives resonate also around 160 ppm.[26b]

Study of the Radical Ion Derivatives. The presence on the same molecule of electron donor and acceptor moieties makes possible the generation of their radical-cation and radical-anion derivatives by oxidation or reduction, respectively (Scheme 2).[36]

In the study of the radical cations of **3** it is necessary to take into account that since molecule **3** has two TTF addends, it is possible to form the monoradical cations and the biradical cations by oxidation of the isomers of **3**. It is interesting to note that if only one of the TTF addends is oxidized, the resulting cation radical is a mixed valence compound, a very attractive species because it can present intramolecular electron transfer through the fullerenic bridge promoted by an external optical or thermal stimulus. In such a case, the different isomers can even present different rates in this process. To study accurately this process, quantitative spectroelectrochemical experiments should be performed, and, in our case, this has not been possible due to the very small amounts of each pure isolated isomer.

The radical cations of bisadducts **3a** (*trans-2*), **3c** (*trans-3*), **3e** (*e*), and **3f** (*cis-3*) were generated by electrochemical oxidation and monitored by EPR and UV-

(35) The other isomers were not obtained pure in enough quantity for determination of a good ^{1}H NMR spectra.

(36) In the cyclic voltammetry in CH_2Cl_2 of the mixture of isomers of **3**, two reversible oxidation processes at 0.67 and 1.14 V (versus Ag/AgCl) corresponding to the TTF's and up to three quasi-reversible reduction processes due to the C_{60} at −0.66 V, −1.02 V, and −1.45 V (versus Ag/AgCl) are observed (see ref 10).

Table 2. NMR Data of Triads 3a (*trans-2*) and 3e (*equatorial*)

	^{1}H chemical shifts (ppm)				^{13}C chemical shifts (ppm)						
	TTF methylenic protons				bridge carbons[a]			adjacent carbons[b]			
isomer	H1	H2	H3	H4	B1	B2	B3	A1	A2	A3	A4
trans-2	4.40–4.60(AB; 15 Hz)		4.35–4.40(AB; 15 Hz)		65.0	64.5	–	153.6	154.4	153.8	160.0
equatorial	3.72(s)	3.98(s)	4.02–4.06(AB; 15 Hz)		65.6	65.2	65.2	154.0	161.0	153.5	154.5

[a] Fullerene Csp^3, bridge carbons between the C$_{60}$ and the TTF. [b] Fullerene Csp^2, carbons adjacent to the bridge ones.
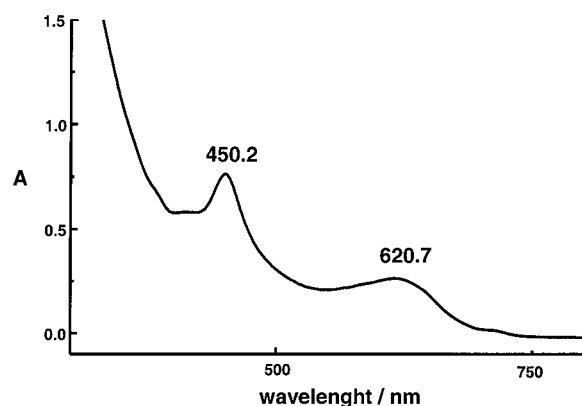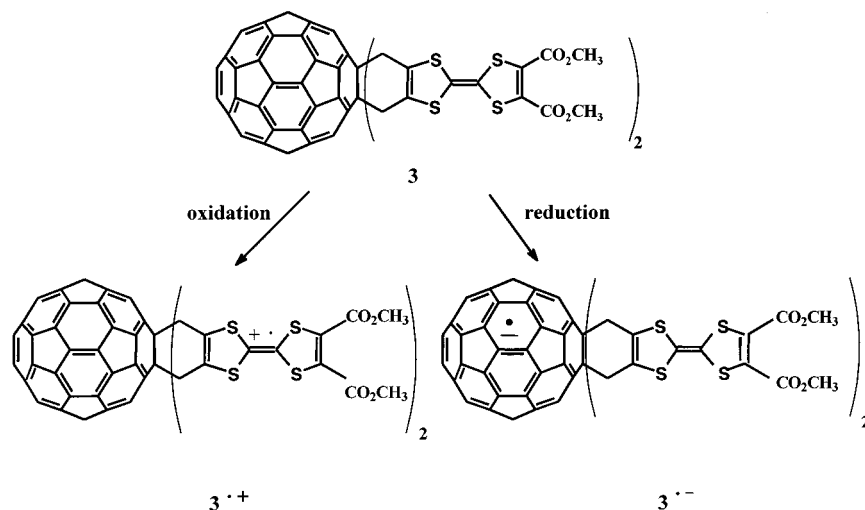
Scheme 2

Figure 4. Visible absorption spectrum of the radical cation obtained from **3a** after 10 min of electrochemical oxidation.

vis spectroscopy. These radical cations have appreciable persistency with lifetimes of the order of days. All show new intense bands in the 400–700 nm region of the electronic spectra (Figure 4), not present in the neutral molecules, which are characteristic of radical cations centered on a TTF core.[37] These absorption bands are very similar to those obtained for the radical-cation derived from the monoadduct **2**.[10] In contrast to the spectra of the neutral compounds, all isomers have almost identical spectra dominated by the characteristic TTF cation radical absorption bands, which appear very intense in the same region where weak bands differentiate the neutral compounds. Although oligothiophenes unexpectedly aggregate when attached to fullerenes,[38] the fact that there are no additional bands in the visible spectra of compounds **3** that could be attributed to dimer

formation is not so surprising if we take into account the appreciable steric hindrance introduced by the bulky fullerene cage, together with the poor solubilities of these compounds that prevent the preparation of highly concentrated solutions, in which aggregation is favored.

The EPR spectra obtained for the cation radicals of **3a** (*trans-2*), **3c** (*trans-3*), **3e** (*equatorial*) and **3f** (*cis-3*) are almost identical (Table 3). All the studies presented below have been performed "in situ" using a flat electrochemical cell adapted to the EPR spectrometer. During the initial steps of the 'in situ' electrochemical oxidation the central signal obtained (Figure 5a) consists of three lines centered at $g = 2.0077(2)$ with relative intensities 1:2:1 very similar to that obtained from the oxidation of the monoadduct **2**.[10] That triplet signal was attributed to the coupling of the free electron to two axial methylenic protons, since the coupling with the equatorial ones is negligible as they lie on the nodal plane of the SOMO. This differentiation is due to the low rate of the boat-to-boat interconversion on the EPR time scale, a situation also present in the case of other C$_{60}$ cycloadducts.[2a,39] We can assume that in the initial steps of the electrochemical oxidation only the monoradical cation is formed. Thus, the fact that the EPR spectra of all the isomers are almost identical to that obtained from the monoadduct **2**, indicates that at room temperature the unpaired electron is in all cases located only on one of the TTF addends. As the electrochemical oxidation proceeds, the EPR spectra changes, and two additional lines start to appear exactly in the middle of the three main lines (Figure 5b). In all the isomers, the spectra of the biradicals develop toward a quintuplet, but we never obtained the theoretical 1:4:6:4:1 relative intensities of the lines expected for

(37) Torrance, J. B.; Scott, B. A.; Welber, B.; Kaufman, F. B.; Seiden, P. E. *Phys. Rev. B* **1979**, *19*, 730.

(38) Apperloo, J. J.; Langeveld-Voss, B. M. W.; Knol, J.; Hummelen, J. C.; Janssen, R. A. J. *Adv. Mater.* **2000**, *12*, 908.

(39) (a) Tago, T.; Minowa, T.; Okada, Y.; Nishimura, J. *Tetrahedron Lett.* **1993**, *34*, 8461. (b) Zhang, X.; Foote, C. S. *J. Org. Chem.* **1994**, *59*, 5235. (c) Fernández-Paniagua, U. M.; Illescas, B.; Martín, N.; Seoane, C.; Cruz, P.; Hoz, A.; Langa, F. *J. Org. Chem.* **1997**, *62*, 3705.

Table 3. EPR Coupling Constants Corresponding to the Radical Species Derived from 3a (*trans-2*), 3c (*trans-3*), 3e (*e*), and 3f (*cis-3*)

isomer	radical anion a_H/G								radical cation a_H/G	
	H1	H2	H3	H4	H5	H6	H7	H8	monoradical	biradical
trans-2	0.18	0.09	0.18	0.10	0.09	0.18	0.18	0.10	1.93	0.95
trans-3	0.07	0.14	0.26	0.10	0.07	0.09	0.26	0.28	1.91	0.94
equatorial	0.00	0.28	0.09	0.21	0.10	0.09	0.09	0.00	1.94	0.96
cis-3	0.28	0.09	0.06	0.05	0.04	0.00	0.29	0.05	1.94	0.95
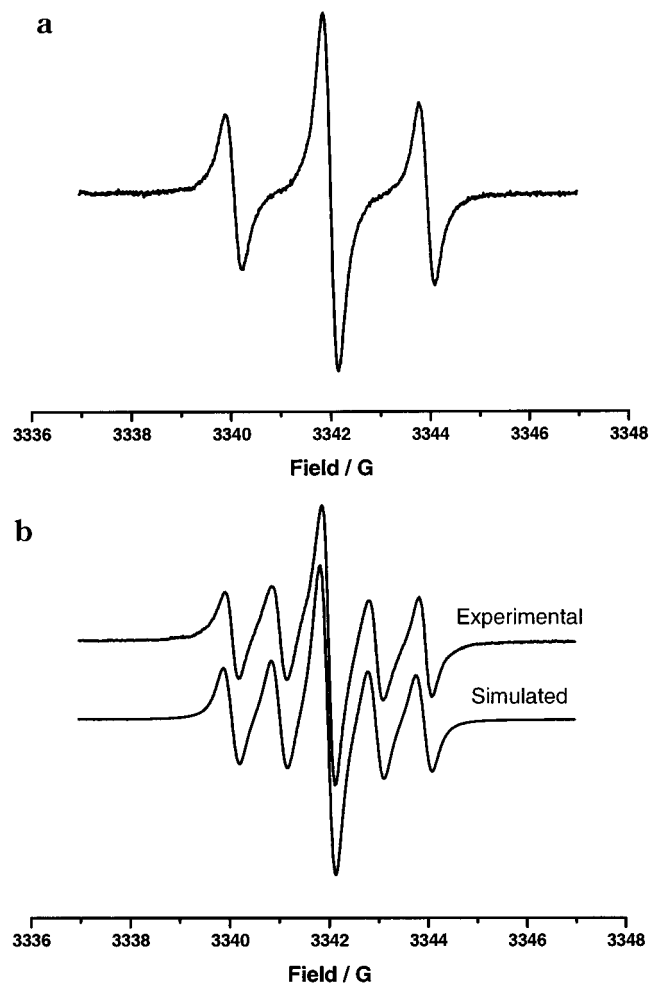
Figure 5. EPR spectra at 293 K in CH_2Cl_2 under isotropic conditions of the radical cation derived from **3c** (*trans-3*) (a) after 5 min of in situ electrochemical oxidation; (b) after 1 h of in situ electrochemical oxidation.

a pure biradical at the fast exchange limit in which the *intramolecular exchange coupling constant* (J^{intra}) between the two electron spins at each TTF addend of the molecule is much bigger than the hyperfine coupling constant with the ^{1}H nuclear spins; i.e., $J^{intra}/g\beta \gg a_H$.[40] Nevertheless, the fact that the line width of the new lines are exactly the same as those of the three already existing lines seems to rule out the possibility of being in the situation in which J^{intra} has an order of magnitude similar to that of the coupling constant a_H.[41] It seems, therefore, that the spectra obtained correspond to the coexistence

of monoradical and biradical species in the solution. Thus, the spectra registered at different oxidation times can be perfectly simulated by the sum, in different proportions, of the spectrum corresponding to the monoradical and that corresponding to the biradical at the fast exchange limit. In Figure 5b, the experimental and simulated EPR spectrum obtained upon oxidation of **3** (isomer *trans-3*) for 1 h is shown; in this case the proportion monoradical:biradical is 1:2. As expected, the coupling constants observed in the biradicals are half those observed for monoradicals (Table 3). On lowering the temperature, we did not observe the $\Delta m_s = 2$ transition of triplet states in any of the biradicals generated. This fact is not surprising since the concentration of the biradical species is always very low, and the distance between the two centers with spin density is long.[42]

Radical anions of isomers **3a** (*trans-2*), **3c** (*trans-3*), **3e** (*e*), and **3f** (*cis-3*) were obtained by electrochemical reduction and were characterized by EPR spectroscopy. As already observed for the anion radical species generated from the mixture of the isomers **3**,[10] the spectra of each isomer show a narrower EPR signal than the one of the radical-anion derived from the monoadduct **2**. This situation permits the observation of the hyperfine structure arising from the coupling of the unpaired electron with the hydrogen atoms of the methylenic groups of the bridges. Therefore, for the first time, the coupling of the electrons of a fulleride with the addend's atoms has been experimentally observed. Contrary to the case of the radical cations, the isomerism does influence the type of signals obtained. Interestingly, it was found that the hyperfine structure of the spectra of the derived radical anions from the above-mentioned isomers are strikingly different to each other. As an example, in Figure 6 we show the experimental and simulated spectra for two of the isomers (**3a**; *trans-2* and **3f**; *cis-3*).

The isotropic coupling constants of the methylenic protons have been calculated and compared with the experimental ones obtained by simulation of the experimental EPR spectra. Due to computational limitations, calculations have been done only for the most stable conformer of each regioisomer in the gas phase. The simulations of EPR spectra were carried out using an iterative least-squares fitting procedure based on Monte Carlo Methods and starting from the B3LYP/3-21G//AM1 calculated proton coupling constants.[43] The results of the simulations are presented in Table 3. The calculated values of the coupling constants are remarkably similar to the experimental ones as can be appreciated on Figure 7, in which the relative experimental coupling constant values are plotted against the calculated ones, and the resulting points of the graph are fitted with a line of slope

(40) Salem, L.; Rowland, C. *Angew. Chem., Int. Engl. Ed.* **1972**, *11*, 92.

(41) (a) Glarum, S. H.; Marshall, J. H. *J. Chem. Phys.* **1967**, *47*, 1374. (b) Brière, R.; Dupeyre, R.-M.; Lemaire, H.; Morat, C.; Rassat, A.; Rey, P. *Bull. Soc. Chim. Fr.* **1965**, *11*, 3290. (c) Hernàndez-Gasio, E.; Mas, M.; Molins, E.; Rovira, C.; Veciana, J.; Borrás-Almenar, J. J.; Coronado, E. *Chem. Mater.* **1994**, *6*, 2398.

(42) Eaton, S. S.; More, K. M.; Sawant, B. M.; Eaton, G. R. *J. Am. Chem. Soc.* **1983**, *104*, 523.
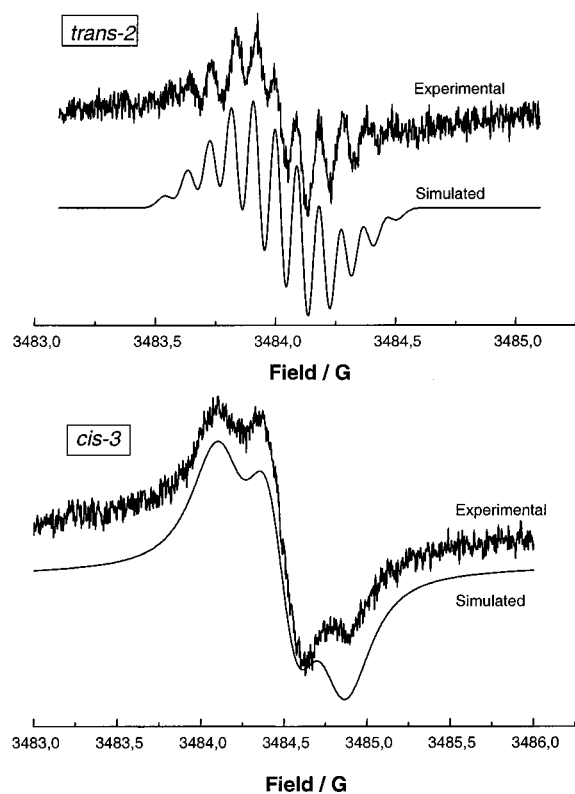
Figure 6. EPR spectra (293 K) in CH$_2$Cl$_2$ under isotropic conditions and simulated EPR spectra of the radical anions derived from **3a** (*trans-2*) and **3f** (*cis-3*).
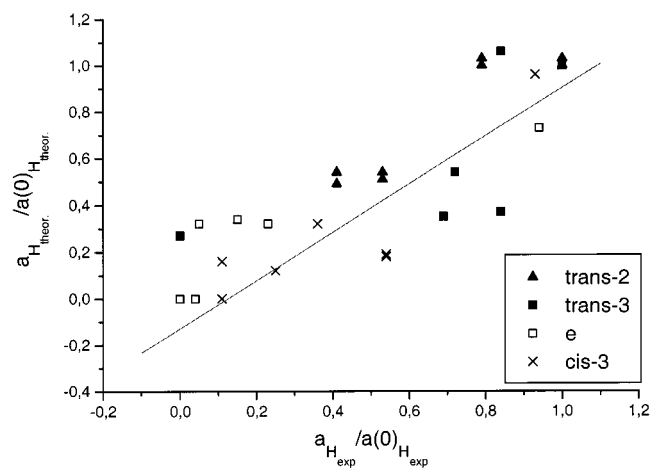
Figure 7. Graphical representation of the relative values of the experimental EPR proton coupling constants versus the calculated ones.

1.03. Therefore, we have shown that the spin density distribution of the anionic species derived from **3** depends strongly on the isomerism, and it has also been shown that the coupling of the unpaired electron with the addend's protons can be predicted by B3LYP/3-21G//AM1 calculations. Thus, the study of the EPR signal of the derived radical anion of C$_{60}$ triads is a potentially extremely useful method for the characterization and assignment of the different isomers.

The experimental values of the hyperfine coupling constants (hfcc's) are excellent proof of the spin density on each nucleus. However, if we want to have an idea of the spin density distribution over the whole molecule, other techniques have to be used. Theoretically, this goal
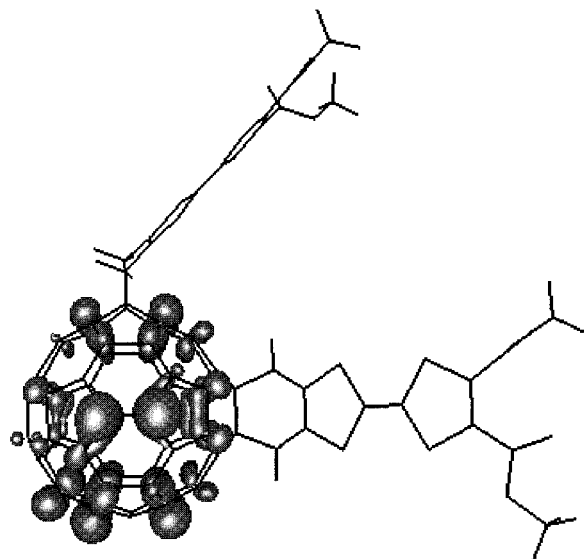
Figure 8. 3D representation of the radical anion spin density of a particular conformer of regioisomer *e* computed at the B3LYP/6-31G**//AM1 level. Isosurface value is 0.001 au.
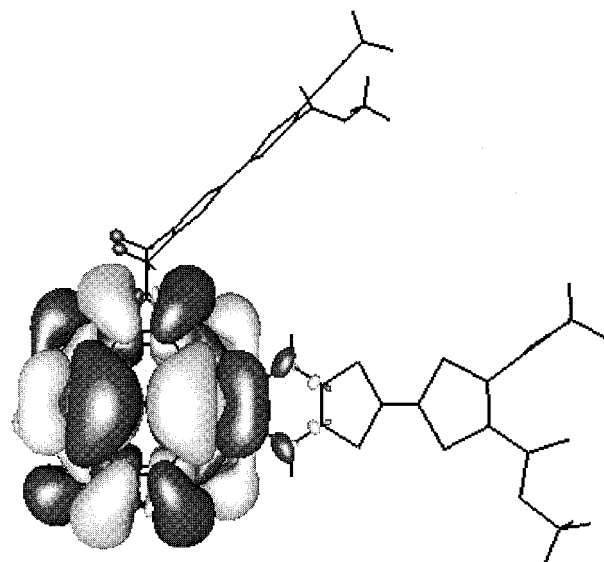
Figure 9. 3D representation of the LUMO of a particular conformer of regioisomer *e* computed at the B3LYP/6-31G**// AM1 level. Isosurfaces values are −0.01 and 0.01 au.

can be achieved through the representation of spin density maps. These maps, which give the value of the spin density at any point of space around the molecule, are calculated by subtracting the electronic density of the α and β electrons. As an example, in Figure 8 the spin density map of a particular conformer of regioisomer *e* computed at the B3LYP/3-21G//AM1 level is presented. Figure 8 shows that the spin density in these species is lower in the region of the fullerene core next to the attached TTF units. Similar results were obtained for the rest of the regioisomers. For the same conformer, Figure 9 depicts the LUMO of the neutral species calculated at the B3LYP/3-21G//AM1 level. It is worth noting that the density of the LUMO orbital of the neutral species differs to some extent from the spin density of the radical anion, although in both cases the amplitude is the highest at the *equatorial* position with respect to the TTF units.

Conclusions

In conclusion, a family of $C_{60}(TTF)_2$ triads has been synthesized and some of the isomers isolated and characterized. In the EPR spectra, it has been seen that there are no differences in the signals obtained for the derived radical cations formed by oxidation of the donor addends. However, by reducing the fullerene cage to obtain the corresponding radical anions, the hyperfine structure of the EPR signal obtained for each isomer shows notable differences. The distinct spin density distribution of the isomers has been studied by density functional calculations and fits with the experimental results. The methodology demonstrated by this study could not only be useful for the characterization of C_{60} triads but also for designing triads with donor addends where charge transfers mediated by the C_{60} can take place.

Experimental Section

Computational Details. Full geometry optimizations without symmetry constraints were carried out with the AM1 semiempirical method[44] as implemented in AMPAC 6.55,[45] a quantum chemistry program from Semichem, Inc. Previous studies have shown that the AM1 method provides reliable results for the geometries and energetics of C_{60},[46] C_{70},[47] and Diels–Alder adducts. AM1 calculations were performed using the restricted formalism. The free energies of formation in gas phase for the different isomers and conformers were calculated from the addition of entropy corrections to the enthalpies of formation. The influence of solvation on the stability of the different species was included by means of self-consistent reaction field methods (SCRF). In particular, SCRF calculations to determine free energies of solvation were performed using the MST model,[48–50] also known as the polarizable continuum model. To simulate the solvent used in HPLC experiments (0.3% of ethyl acetate in methylene chloride) we used the parametrization of the MST/SCRF continuum model corresponding to a chloroform solution.[48,49] The reasons for this choice are that the methylene chloride solvent has not been parametrized yet at the semiempirical AM1 level, and that chloroform and methylene chloride have a similar dielectric constant. Free energies of solvation in chloroform were computed with the AM1 method with a modified version of the MOPAC computer program.[51]

The averaged dipole moment of each regioisomer was obtained by considering a Maxwell–Boltzmann distribution of its conformers and using their Gibbs computed energies at 298 K in solution, that is:

$$\langle \mu_k \rangle = \sum_{i=1}^{n_k} p_i \mu_i \text{ with } p_i = \frac{g_i \exp\left(-\dfrac{\Delta G_i^o}{RT}\right)}{\sum_{i=1}^{n_k} g_i \exp\left(-\dfrac{\Delta G_i^o}{RT}\right)}, \quad (1)$$

where n_k is the total number of conformers of regioisomer k,

and g_i, μ_i, and ΔG_i^o are the degeneration, the dipole moment, and the sum of the formation and solvation Gibbs energies, respectively, of conformer i belonging to regioisomer k.

For selected systems we have calculated the isotropic hyperfine coupling constants (hfcc) of the methylenic hydrogen atoms of the cyclohexene bridges between the C_{60} and the TTF addend from the electron spin densities at the hydrogen atom using the following equation,

$$a_H = \frac{8\pi}{3} \frac{g_e}{g_o} \gamma_H \beta_H \rho_s(\mathbf{r}_H) \quad (2)$$

where g_e/g_o is the ratio of the isotropic g value for the radical to that of the free electron, γ_H and β_H are the gyromagnetic nuclear ratio and the nuclear magneton, respectively, for the hydrogen atom, and $\rho_s(\mathbf{r}_H)$ is the spin density on the nucleus of the hydrogen atom considered. The approach we use to evaluate these quantities is the density functional theory in the unrestricted Kohn–Sham (UKS) version.[52] In particular, hfcc's were calculated using the B3LYP[53] density functional with the 3-21G basis set[54] and employing the AM1-optimized geometries of the radical anions (B3LYP/3-21G//AM1). For all radical anions, the S^2-value (where S represents the electronic spin) over the reference Slater determinant of self-consistently converged Kohn–Sham orbitals is very close to the theoretical value for a doublet state (0.75), being always smaller than 0.7552. The isotropic hyperfine coupling constants of free radicals are one of the most challenging one-electron properties for ab initio quantum mechanical methods. Good results are generally found using the B3LYP density functional and basis sets which describe well the core region of the electron density.[55] One can expect that the B3LYP/3-21G//AM1 method will provide at least qualitatively correct hfcc's that can be used to compared hfcc's of different regioisomers. Comparison with experiment (vide supra) reinforces this point. The isotropic hyperfine coupling constants were calculated with the help of the Gaussian-98 program.[56]

General Procedures. All cycloaddition reactions were performed under inert atmosphere and in the absence of light. Materials and solvents were obtained from commercial suppliers. C_{60} was purchased from MER corporation (Tucson, AZ). Compounds **1** and **2** were prepared as described in the literature.[10,57]

Instruments. UV-vis: Varian Cary 5; EPR: X-Band Bruker ESP 300 E, equipped with a temperature controller ER 412HT, a field frequency (F/F) lock accessory and built-in NMR

(43) Kriste B. EPRFTSM Program, Freie Universität Berlin, 1991; *J. Magn. Reson.* **1987**, *73*, 213

(44) Dewar, M. J. S.; Zoebisch, E. G.; Healy, E. F.; Stewart, J. J. P. *J. Am. Chem. Soc.* **1985**, *107*, 3902.

(45) AMPAC 6.55, 1997 Semichem, 7204 Mullen, Shawnee, KS 66216.

(46) Solà, M.; Mestres, J.; Martí, J.; Duran, M. *Chem. Phys. Lett.* **1994**, *231*, 325.

(47) Mestres, J.; Duran, M.; Solà, M. *J. Phys. Chem.* **1996**, *100*, 7449.

(48) Luque, F. J.; Bachs, M.; Orozco, M. *J. Comput. Chem.* **1994**, *15*, 847. Bachs, M.; Luque, F. J.; Orozco, M. *J. Comput. Chem.* **1994**, *15*, 446. Orozco, M.; Bachs, M.; Luque, F. J. *J. Comput. Chem.* **1995**, *16*, 563.

(49) Luque, F. J.; Zhang, Y.; Aleman, C.; Bachs, M.; Gao, J.; Orozco, M. *J. Phys. Chem.* **1996**, *100*, 4269.

(50) (a) Miertuš, S.; Scrocco, E.; Tomasi, J. *Chem. Phys.* **1981**, *55*, 117. (b) Tomasi, J.; Persico, M. *Chem. Rev.* **1994**, *94*, 2027.

(51) Stewart, J. J. P. MOPAC6, QCPE 455, Indiana University. Bloomington, IN 1993.

(52) (a) Hohenberg, P.; Kohn, W. *Phys. Rev. A* **1964**, *136*, 864. (b) Kohn, W.; Sham, V. *Phys. Rev. A* **1965**, *140*, 1133.

(53) (a) Becke, A. D. *J. Chem. Phys.* **1993**, *98*, 5648. (b) Lee, C.; Yang, W.; Parr, R. G. *Phys. Rev. B* **1988**, *37*, 785. (c) Stevens, P. J.; Devlin, F. J.; Chablowski, C. F.; Frisch, M. J. *J. Phys. Chem.* **1994**, *98*, 11623.

(54) (a) Binkley, J. S.; Pople, J. A.; Hehre, W. J. *J. Am. Chem. Soc.* **1980**, *102*, 939. (b) Gordon, M. S.; Binkley, J. S.; Pople, J. A.; Pietro, W. J.; Hehre, W. J. *J. Am. Chem. Soc.* **1982**, *104*, 2797.

(55) (a) Adamo, C.; Barone, V.; Fortunelli, A. *J. Phys. Chem.* **1994**, *98*, 8648. (b) Barone, V.; Bencini, A.; di Mateo, A. *J. Am. Chem. Soc.* **1997**, *119*, 10831. (c) Cirujeda, J.; Vidal-Gancedo, J.; Jürgens, O.; Mota, F.; Novoa, J. J.; Rovira, C.; Veciana, J. *J. Am. Chem. Soc.* **2000**, *122*, 11393.

(56) Frisch, M. J.; Trucks, G. W.; Schlegel, H. B.; Scuseria, G. E.; Robb, M. A.; Cheeseman, J. R.; Zakrzewski, V. G.; Montgomery, J. A.; Stratmann, R. E.; Burant, J. C.; Dapprich, S.; Milliam, J. M.; Daniels, A. D.; Kudin, K. N.; Strain, M. C.; Farkas, O.; Tomasi, J.; Barone, V.; Cossi, M.; Cammi, R.; Mennucci, B.; Pomelli, C.; Adamo, C.; Clifford, S.; Ochterski, J.; Petersson, G. A.; Ayala, P. Y.; Cui, Q.; Morokuma, K.; Malick, D. K.; Rabuck, A. D.; Raghavachari, K.; Foresman, J. B.; Cioslowski, J.; Ortiz, J. V.; Stefanov, B. B.; Liu, G.; Liashenko, A.; Piskorz, P.; Komaromi, I.; Gomberts, R.; Martin, R. L.; Fox, D. J.; Keith, T. A.; Al-Laham, M. A.; Peng, C. Y.; Nanayakkara, A.; Gonzalez, C.; Challacombe, M.; Gill, P. M. W.; Johnson, B. G.; Chen, W.; Wong, M. W.; Andres, J. L.; Head-Gordon, M.; Replogle, E. S.; Pople, J. A. Gaussian Inc., Pittsburgh, PA, 1998.

(57) Llacay, J.; Mata, I.; Molins, E.; Rovira, C.; Veciana, J. *Adv. Mater.* **1998**, *10*, 330.

gaussmeter; LDI-TOF: Kratos Kompact Maldi 2 K-probe (KRATOS Analytical) operating with pulsed extraction of the ions; ^{1}H NMR and ^{13}C NMR: Bruker AC 400 and a Bruker Aspect 3000; HMBC NMR: VXR-500S Spectrometer; HPLC: Shimadzu SCL-10A VP, KROMASIL 100 Si 5 μm (Analytical HPLC: Spherisorf 25 × 0.46 cm, 20 μL; Preparative HPLC: Spherisorf 25 × 1.0 cm, 500 μL).

Bis[1,2-(cyclohexenylbismethoxycarbonyltetrathia-fulvalene)]-buckminster- fullerene 3. Method A. To a refluxing solution of 73.6 mg (0.1 mmol) of C$_{60}$ in toluene was added a solution of 41 mg (0.1 mmol) of compound **1** in 8 mL of benzonitrile, and the resulting solution was refluxed for 1 h. The solvent was evaporated and the residue chromatographed (silica gel, CS$_2$–CH$_2$Cl$_2$) to give unreacted C$_{60}$ (15 mg, 20.4% from the initial C$_{60}$), 60 mg of monoadduct **2** (69.1% from reacted C$_{60}$), and 33 mg of a mixture of bisadducts **3** (28.7% from reacted C$_{60}$).

Method B. A solution of 200 mg (0.18 mmol) of monoadduct **2** and 38 mg (0.09 mmol) of compound **1** in 40 mL of cholorobenzene was refluxed for 1 h. The solvent was evaporated and the residue chromatographed (silica gel, CH$_2$Cl$_2$) to give 124 mg of unreacted monoadduct (62% from initial monoadduct **2**) and 58 mg of a mixture of bisadducts **3** (57.7% from reacted monoadduct **2**).

FT-IR (KBr) υ (cm^{-1}) 1734, 1576, 1433, 1258, 1090, 1026, 766, 527; UV-vis (CH$_2$Cl$_2$) λ_{max}(log ϵ) 257 (4.96), 310 sh. (4.72), 418 sh. (3.88), 450 sh. (3.77), 675–750 broad band (1.30); HRMS calcd for C$_{84}$H$_{20}$O$_8$S$_8$ m/z 1411.892, found 1411.892; LDI-TOF-MS 1412 [M$^+$]; ^{1}H NMR (300 MHz, CS$_2$–CD$_2$Cl$_2$ 1:2) δ (ppm) 4.31–4.25 (m, broad), 3.91–3.87 (m).

Generation of Radical Cations and Anions Derived from 3. Radical cations were obtained by in situ electrochemical reduction, monitored by an EG&G PAR 263A potentiostat/galvanostat, on an EPR cell equipped with Pt wires as working and counter electrodes and using the Ag/AgCl system as a reference electrode. Experimental conditions for the electrochemical generation of radical cations was as follows: +0.8 V, CH$_2$Cl$_2$ 0.2 M in Bu$_4$NPF$_6$. Experimental conditions for the electrochemical generation of radical anions was as follows: −0.8 V, CH$_2$Cl$_2$ 0.2 M in Bu$_4$NPF$_6$.

Supporting Information Available: Complete computational details in the form of Z-matrixes for the theoretical studies carried out for isomers of **3**. This material is available free of charge via the Internet at http://pubs.acs.org.

JO010748F